Chaos and mixing in a geostrophic flow

Robert P. Behringer,[a] Steven D. Meyers, and Harry L. Swinney
Department of Physics and Center for Nonlinear Dynamics, The University of Texas at Austin, Austin, Texas 78712

(Received 28 August 1990; accepted 22 January 1991)

Experiments on Rossby waves on an azimuthal jet in a rapidly rotating annular tank reveal a striking barrier to mixing across the jet. A model based on the experiments assumes a two-dimensional incompressible flow described by a time-dependent streamfunction consisting of azimuthally propagating waves on a narrow jet. When there is only one wave, all Lagrangian particle trajectories are closed in the appropriate reference frame. When two independent waves are present, some trajectories are chaotic, and the size of the chaotic sea grows as the amplitude of the second wave is increased; however, at least one barrier to global transport—an invariant surface—prohibits trajectories from crossing the jet. The addition of a third wave is found to break the barrier only if the wave amplitudes exceed the width of the jet. In the experiment, the wave amplitude is typically about one-half the jet width, and the barrier to mixing persists even at the highest accessible Reynolds numbers.

I. INTRODUCTION

Associated with the appearance of Rossby waves are barriers to mixing in the atmosphere and oceans. An example of particular current interest is the polar night jet that surrounds the ozone depleted region above Antarctica.[1]

The present study considers mixing in a simple Rossby wave flow in a rotating annular geometry (Fig. 1) that can be well controlled in laboratory experiments. An azimuthal jet is produced by the action of the Coriolis force on radially pumped fluid. The annulus rotates rapidly so that the Rossby number for the jet is 0.03 to 0.15, comparable to Rossby numbers of planetary flows.[2] Experiments on Rossby waves in the rotating annulus reveal a striking barrier to transport, as Fig. 2 illustrates. Dye injected on one side of the jet rapidly mixes with fluid on the same side of the jet, but after 500 rotations of the tank, the dye has not crossed the jet. Even after 2000 rotations of the tank, little mixing has occurred.

The flow is incompressible and, by the Taylor–Proudman theorem, essentially two dimensional. Hence the velocity field can be expressed in terms of a streamfunction $\psi(r,\theta,t)$: $u_r = -r^{-1}\,\partial\psi/\partial\theta$ and $u_\theta = \partial\psi/\partial r$. The Lagrangian trajectory $[r(t),\theta(t)]$ of a particle is given by

$$\frac{dr}{dt} = -r^{-1}\frac{\partial\psi}{\partial\theta} \tag{1}$$

and

$$\frac{d\theta}{dt} = r^{-1}\frac{\partial\psi}{\partial r}. \tag{2}$$

We are concerned here with the behavior of tracer particles in velocity fields that are periodic or multiperiodic, not chaotic. As is well known, particles in a regular (nonchaotic) Eulerian velocity field can have chaotic trajectories, a situation called Lagrangian turbulence or chaotic advection.[3]

Chaotic advection has been studied for a number of simple closed systems, including the blinking vortex, journal bearing flow, and cavity flow.[4] Those studies were conducted at low Reynolds number, typically less than unity, well below the onset of the first instability in the Eulerian velocity field.[5] In our study the Reynolds number is in the range 10^3 to 5×10^4, well beyond the primary instability at which there is a transition from an axisymmetric jet to a jet with Rossby waves. Another important difference between previous studies of chaotic advection and the present study is that most previous studies were made on periodically forced flows,[4,5] while in our system the forcing (pumping of fluid) is time independent. The time dependence of our flow arises from the naturally occurring azimuthal waves.

We consider the mixing properties for an Eulerian velocity field that is taken as given. The solution of the Navier–Stokes equation for our geometry and forcing conditions is a difficult problem to be addressed in the future. Even in the previous experiments on low Reynolds number flows,[4] solutions for the streamfunction were often not known, or if the velocity field was known, it could not be integrated analytically to obtain particle trajectories; thus insight into mixing properties has often been gained by analyzing experiments and simple models. In our study the basic question is the following: Does a simple model for the streamfunction, drawn from experimental observations, yield a robust barrier to transport as observed in the experiments? The answer is yes. Such a barrier can be viewed as an invariant surface (KAM torus) in a Hamiltonian system with Hamiltonian ψ. In the atmosphere or ocean such an invariant surface could provide an essentially impervious barrier to particle transport. This suggests that the tools of KAM theory could be exploited to gain insight into mixing in planetary type flows.

The barrier to mixing revealed by our experiments differs from the barriers found in most previous systems studied,[4] where barriers dividing the flow into two separate regions were not generally observed.[6] The persistence of the barrier to global mixing that we have found when the flow is multiperiodic and the wave amplitude is large was unexpect-

[a] Permanent address: Department of Physics and Center for Nonlinear Studies, Duke University, Durham, North Carolina 27706.

 0899-8213/91/051243-07$02.00

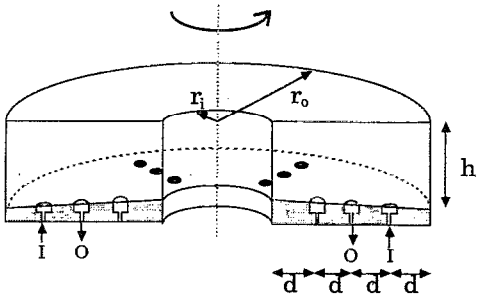

FIG. 1. A cross section of the tank used to conduct the experiments. The working basin, a rigid annulus with a sloping bottom and a flat lid, has an inner diameter of 21.6 cm and an outer diameter of 86.4 cm. The depth increases from 17.1 cm at the inner radius to 20.3 cm at the outer radius; thus the conical bottom has a slope $s = -0.1$. The rotation rate Ω ranges from 0 to 25 rad/sec. Fluid is pumped through ports in the bottom of the tank; the arrows indicate the pattern of inlets (I) and outlets (O) used in the present experiments. The radial distance d between the ports is 8.1 cm.

ed, while the rapid mixing that we observe to either side of the jet is similar to that found in previous studies. We are concerned here with nonchaotic Eulerian velocity fields, but we should mention that even at high Reynolds number ($\sim 10^4$) where the velocity field is chaotic, we observe that the barrier to mixing persists.

II. EXPERIMENTS

The rotating annulus (Fig. 1) has a sloping bottom that mimics the atmospheric latitudinal gradient in the Coriolis force (the β effect), with a β coefficient given by $\beta = 2\Omega s/\bar{h}$, where $\bar{h}$ is the mean depth of the tank and s is the slope of the bottom.[7–9] A corotating jet was produced by the action of the Coriolis force on fluid pumped radially inward from a set of six outlets located on the bottom of the tank at a common radius to a set of six inlets at a smaller radius. The ports at each radius were uniformly spaced azimuthally and positioned so that for each inlet there was an outlet along the same radius. The azimuthal velocity of the jet was typically two orders of magnitude larger than the the radial velocity from the pumping. The velocity field was determined with respect to the rotating annulus by measuring the length of particle streaks in time exposure photographs obtained with a camera that was corotating with the annulus.[7,8]

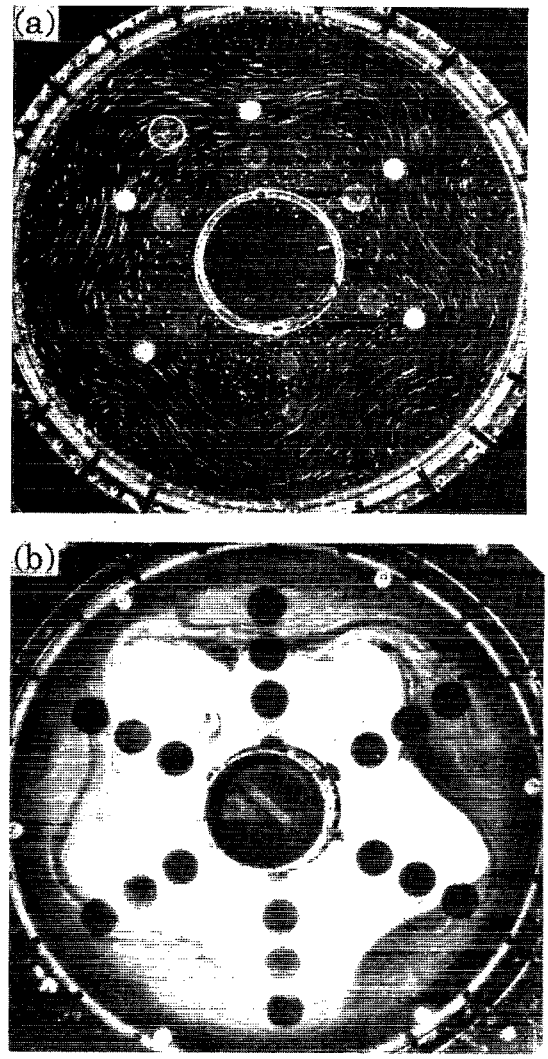

FIG. 2. (a) Particle streak photograph showing the local velocity field, revealing the presence of Rossby waves. (b) A dye photograph showing the barrier to mixing between the inner and outer parts of the tank. Dye was injected in the outer part of the tank after the flow was well established. Five hundred tank rotations after the dye injection, nearly complete mixing has occurred in the outer region of the tank, but almost no dye has penetrated to the inner region, except for the small tongues that rapidly carry small amounts of fluid across the jet. The dominant wave number in this case is $m_1 = 5$. The parameters for (a) are $\Omega = 12.5$ rad/sec; F, the total pumping rate, is 137 cm^3/sec; Ro = 0.039; and Re = 7000. In (b) $\Omega = 18.8$ rad/sec, $F = 90$ cm^3/sec, Ro = 0.038, and Re = 7990.

III. MODEL

We model the flow with a streamfunction based on experimental observations: (i) The measured radial dependence of the azimuthal component of the velocity for Reynolds numbers $O(10^4)$, as in the present experiments, has the form $\mathrm{sech}^2[(r-\bar{r})/L]$, where L and $\bar{r}$ are, respectively, the measured values of the width and mean radial position of the jet.[9] Hence the streamfunction has the tanh form. (ii) Fourier transforms of the azimuthal component of the velocity indicate that there are at least two azimuthal modes in the parameter range of the experiment: a dominant mode [with *five* waves in the examples in Figs. 2 and 3(a)] and one or more weaker modes [with three and six waves in Figs. 2 and 3(a)]. Thus the streamfunction has the assumed form

$$\psi = LU_0 \sum_{j=1}^{3} \epsilon_j \left[\tanh\left(\frac{\{r - \bar{r} - b\cos[m_j(\theta - \omega_j t)]\}}{L} \right) \right], \tag{3}$$

where $\Sigma_j \epsilon_j = 1$, U_0 is the maximum possible velocity, and ω_j is the azimuthal wave speed (measured with respect to the rotating annulus) of the mode with m_j waves.

At the inner and outer walls of the rotating annulus the

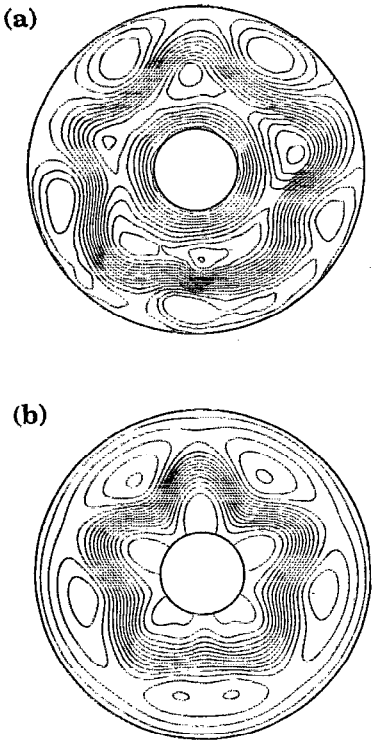

FIG. 3. (a) Contour plot of streamlines deduced from a particle streak photograph of the flow with $b/L = 0.55$, $L = 7.1$ cm, $\Omega = 12.5$ rad/sec, $F = 110$ cm^3/sec, Ro $= 0.042$, and Re $= 5600$. (b) Contour plot of streamlines for the model streamfunction (3) with two waves, for parameter values $b/L = 0.55$ cm, $L = 7.1$ cm, $\epsilon_1 = 0.83$, $\epsilon_2 = 0.17$, $\epsilon_3 = 0$, $m_1 = 5$, $m_2 = 4$, $\omega_1 = 0.1$ rad/sec, and $\omega_2 = 0.168\,03$ rad/sec. In both (a) and (b) the contour intervals are 8 cm^2/sec, and the largest ψ contour (inside the five large outer islands) is 25 cm^2/sec.

velocity field given by (3) is small but nonzero; thus it satisfies neither the impenetrable boundary condition nor the no-slip boundary condition. We have examined several modified forms of (3) that satisfy the boundary conditions at the walls and have found that our results for the mixing properties of the flow are insensitive to the particular form of the modification. In most of the simulations presented here, the narrow boundary layer is accounted for by multiplying the argument of the tanh function by $g(r) = 1 + h(r)$, where $h(r)$ is approximately zero, except in the boundary layer, where it diverges:[10]

$$h(r) = 1 + [(\lambda(r_o - r_i)/(r - r_i)(r_o - r)]^4. \tag{4}$$

Here r_i and r_o are, respectively, the inner and outer radii of the annulus, and λ characterizes the boundary layer thickness. With $h(r)$ as a factor in the argument, the tanh function approaches $+1$ at the outer boundary and -1 at the inner boundary. For a Stewartson boundary layer the thickness is[2] $[(\nu/\Omega)^{1/2}\bar{h}]^{1/2}$, which is typically 0.6 cm in our experiments (ν is the kinematic viscosity). Again, we emphasize that our *ad hoc* form for the boundary layer was chosen for convenience since our results for the mixing were found to be insensitive to the shape of the boundary layer.

If only one wave were present in the streamfunction, say the one subscripted 1, then the particle trajectories would necessarily be regular, as can be seen by changing to a set of coordinates moving with the wave speed ω_1. That is, if we transform to a new set of polar coordinates (r,ϕ) in which r is unchanged, and

$$\phi = \theta - \omega_1 t, \tag{5}$$

then the streamfunction becomes

$$\psi'(r,\phi,t) = U_0 L\,[\epsilon_1 \tanh\{[r - \bar{r} - b\cos(m_1\phi)]/L\} + \epsilon_2 \tanh(\{r - \bar{r} - b\cos[m_2(\phi - \delta\omega_2 t)]\}/L) + \cdots] - \omega_1 r^2/2, \tag{6}$$

where $\delta\omega_j = \omega_j - \omega_1$. Then, the time evolution of polar coordinates for a fluid particle is given by

$$\frac{dr}{dt} = -r^{-1}\frac{\partial\psi'}{\partial\phi} \tag{7}$$

and

$$\frac{d\phi}{dt} = r^{-1}\frac{\partial\psi'}{\partial r}. \tag{8}$$

In the remainder of this work we will consider flows (which will contain two or three waves) in the (r,ϕ) frame, in which the primary wave is stationary.

A last point concerns an additional connection to Hamiltonian dynamics. If the Hamiltonian H is defined in terms of any streamfunction $\psi(x,y,t)$ by

$$H(x,y,\alpha,p_\alpha) = \psi(x,y,\alpha) + p_\alpha, \tag{9}$$

then the equations of motion for the Lagrangian coordinates and the newly introduced momentum p_α and its conjugate generalized coordinate α form an autonomous Hamiltonian system that is identical to the original time-dependent streamfunction equations (1) and (2), and H is a constant of the motion. This justifies the use of the machinery of Hamiltonian dynamics, and in particular the concepts developed to describe the breakup of invariant surfaces as some parameter passes through a critical value.[11,12] In the original streamfunction formulation, trajectories evolve in the three space (x,y,t). In the Hamiltonian description, trajectories evolve in a four-dimensional space (x,y,α,p_α), but the constraint $H = \text{const}$ yields trajectories in (x,y,α) space that are identical to those in (x,y,t) space. An invariant surface isolates one region of (r,ϕ,α) space [or (r,ϕ,t) space] from the remainder.[13]

IV. RESULTS

Some examples of the experimental parameters on which the model calculations were based are given in Table I. The principal observation is that there exists a barrier to mixing even at the highest Reynolds numbers accessible in our experiments. The viscous dissipation (Ekman) time, typically 30 sec,[8] is long compared to the time required for mixing on either side of the jet, yet the barrier to mixing across the jet persists for much longer times, even thousands of seconds (cf. the rotation period of the tank, typically 0.25 sec). Typical values for b/L were 0.6; for ϵ_1, 0.6; for ϵ_2 and ϵ_3, 0.1–0.3. Our analysis of streak photographs yields the instantaneous velocity field but no information on the time evolution of the velocity.

Using a standard Runge–Kutta algorithm, we have numerically integrated (7) and (8) for the coordinates (r,ϕ) of fluid particles in the frame of the first wave. In Fig. 4 we show a series of Poincaré sections for the case of two waves. These sections were obtained by strobing the trajectories at times $t_s = 2\pi/\delta\omega_2$. For ϵ_2 small enough, most trajectories appear regular over a long period of time. However, as ϵ_2

TABLE I. Values of parameters for three experimental runs with different principal wave numbers m_1. Run 2 with $m_1 = 5$ is illustrated in Fig. 2(b). The total rate of fluid pumped through the ports is given by F. The Reynolds number and Rossby number are given, respectively, by $\mathrm{Re} = U_0 L/\nu$, where ν is the kinematic viscosity, and $\mathrm{Ro} = U_0/2\Omega L$.

	Run 1	Run 2	Run 3
m_1	4	5	6
m_2	8	3	5
m_3	3	6	7
ϵ_1	0.64	0.64	0.59
ϵ_2	0.18	0.18	0.29
ϵ_3	0.18	0.18	0.12
Ω (rad/sec)	25.1	18.8	25.1
F(cm^3/sec)	350	90	90
U_0 (cm/sec)	47.3	10.1	28.3
L (cm)	7.8	7.1	6.3
b/L	0.58	0.55	0.46
Re	40 900	7990	19 700
Ro	0.12	0.038	0.090

becomes larger, the size of the chaotic region increases, and the closed orbits in the Poincaré sections are increasingly replaced by chaotic seas. However, even for two waves of equal streamfunction amplitude, there remains a barrier between the inner and outer parts of the annulus, as seen in Fig. 4(d). An issue that is not currently resolved is whether any chaotic trajectories exist for arbitrarily small secondary wave amplitudes.

Figure 5 illustrates the transition from a regular to a chaotic particle trajectory for a particle initially just outside the center of the jet. As ϵ_2 grows, the time series becomes multiply periodic and then chaotic.

In the experiment we have not observed b/L values larger than about 0.6. Neither the experiment nor the model (with parameters deduced from experiment) yield rapid global mixing for quasiperiodic flows. Even at large Reynolds number, where the Eulerian velocity field becomes nonperiodic and there is wave breaking, rapid global mixing is not observed in the experiments. In this regime the model is clearly inadequate. However, as a guide to future experiments, we have explored the behavior of the model for b/L values well beyond those observed, to see how large b/L must be for rapid global mixing to occur. In this exercise we take b/L to have the same value for all three waves; very likely b/L has different values for the different modes, but b/L has been determined only for the total jet, not for the individual modes. We have found global mixing in the model only for three waves with $b/L > 1$; global mixing was not found with only two waves, even with $b/L = 1.2$, far beyond the observed value. The onset and growth of leakage across the final barrier with increasing b/L is illustrated in Fig. 6. For $b/L < 1$, no leakage across the final barrier was found for any ϵ_2 and ϵ_3. For $b/L > 1$, leakage across the barrier occurred as ϵ_2 and ϵ_3 were increased. The largest observed leakage for $b/L \approx 1$ was for $\epsilon_1 = 0.77$, $\epsilon_2 = 0.15$, and $\epsilon_3 = 0.08$; further increases in ϵ_2 and ϵ_3 led to a decrease in leakage across the barrier, which is not entirely understood.

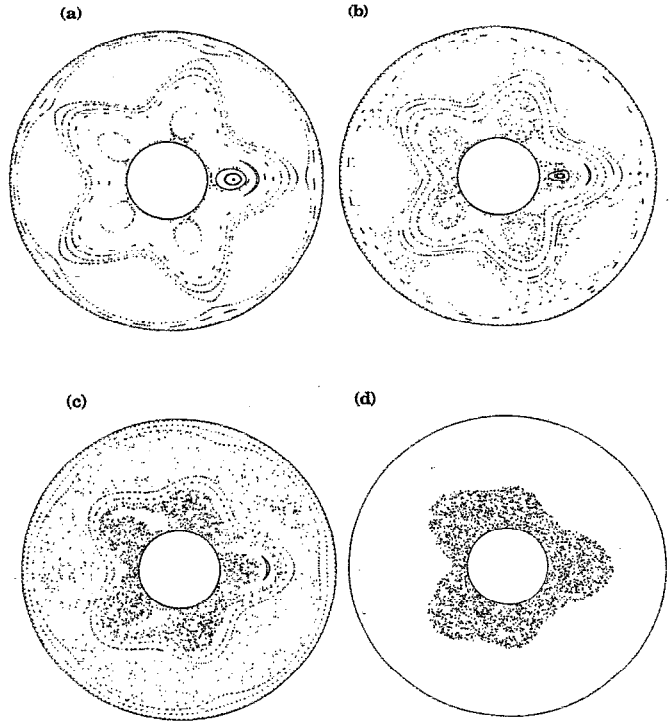

FIG. 4. Poincaré sections for the model with two waves for increasing amplitude of the second wave: (a) $\epsilon_1 = 0.99$, $\epsilon_2 = 0.01$; (b) $\epsilon_1 = 0.91$, $\epsilon_2 = 0.09$; and (c) $\epsilon_1 = 0.67$, $\epsilon_2 = 0.33$. Each Poincaré section shows results generated from 15 particles initially equally spaced along a radial line at $\phi = 0$. The isolating surface for the case $\epsilon_2 = 0.50$ is clear in the Poincaré section in (d) $\epsilon_1 = 0.50$, $\epsilon_2 = 0.50$, where the trajectories were generated for 15 particles initially in the inner region equally spaced in azimuth at $r = 12.0$ cm. In all cases b/L was 0.55, and the elapsed time was 10^4 sec.

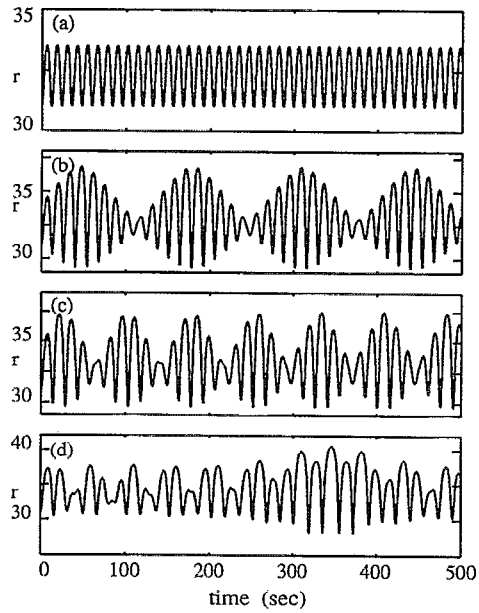

FIG. 5. Time series showing the onset of chaos in the Lagrangian trajectory of a fluid particle as the secondary wave grows in amplitude. (a) $\epsilon_1 = 1.0$, $\epsilon_2 = 0$; (b) $\epsilon_1 = 0.95$, $\epsilon_2 = 0.05$; (c) $\epsilon_1 = 0.91$, $\epsilon_2 = 0.09$; and (d) $\epsilon_1 = 0.83$, $\epsilon_2 = 0.17$. In all cases $U_0 = 20$ cm/sec, $b/L = 0.55$, $L = 7.1$ cm, and the initial position is $r = 31.0$ cm, $\phi = 0.628$.

For $b/L < 1$ many trajectories on either side of the core of the jet are chaotic, but if a trajectory begins in the inner (outer) part of the tank it always remains in the inner (outer) part of the tank. For instance, Fig. 6(a) for $b/L = 0.9$ shows a Poincaré section for 15 trajectories all initially in the inner region; no trajectories reach the outer region, even after 5000 sec. However, for $b/L > 1$ there is appreciable diffusion of trajectories across the former barrier in a relatively short time, as seen in Fig. 6(c), where $b/L = 1.1$. Figure 6(b) shows the intermediate case $b/L = 1$; after a long time some of the trajectories have crossed the barrier. However, our ability to quantify the rate of global mixing for $|(b/L)| \simeq 1$ was limited by numerical error.

Capturing the details of how the trajectories cross the remnants of the last isolating surface is beyond the scope of the present work. However, we can estimate the average rate at which trajectories move across the final barrier as follows. Let $n_i(t)$ and $n_o(t)$ be the number of members of a large ensemble of trajectories that are, respectively, "inside" and "outside" the remnants of the last isolating surface. [Such a surface is approximately given by the outer boundary of the points in Fig. 6(a).] We expect that for a large ensemble, n_i and n_o will approach steady values as t approaches infinity, regardless of the initial values $n_i(0)$ and $n_o(0)$. We estimate the dynamics of the approach to steady populations by the equations

$$\frac{dn_i}{dt} = \left(\frac{f_o}{\tau}\right) n_o - \left(\frac{f_i}{\tau}\right) n_i \tag{10}$$

and

$$\frac{dn_o}{dt} = \left(\frac{f_i}{\tau}\right) n_i - \left(\frac{f_o}{\tau}\right) n_o. \tag{11}$$

Here, τ is some characteristic time for the "diffusion" across the barrier. The quantities f_o and f_i are $O(1)$ quantities reflecting the relative phase space volumes "inside" and "outside" the surface. The solution of these equations is easily obtained and consists of an exponential relaxation toward steady state populations given by

$$n_o(\infty)/n_i(\infty) = f_i/f_o, \tag{12}$$

and

$$n_o(\infty) + n_i(\infty) = n_o(0) + n_i(0). \tag{13}$$

The relaxation time for this process is

$$T = \tau/(f_i + f_o). \tag{14}$$

We have estimated the time scale T for $b/L = 1.2$, $\epsilon_1 = 0.77$ $\epsilon_2 = 0.08$, and $\epsilon_3 = 0.15$ by studying the Poincaré sections for 60 trajectories. The initial positions of these trajectories are distributed uniformly in ϕ at the radius $r = 12$ cm, well inside the remnant of the last isolating curve. Thus $n_o(0) = 0$, and $n_i(0) = 60$. We counted the number of points

$$N_o(t) = n_o(t_s) + n_o(2t_s) + n_o(3t_s) + \cdots + n_o(t) \tag{15}$$

in each Poincaré section lying outside the former isolating curve, as estimated from a Poincaré section with $b/L = 1.0$. Here t_s is the strobe time of the Poincaré section. Typically, $N_o(t)$ is an increasing function of time. In practice it is easier to determine

$$\Delta N_o(t, t_{\text{obs}}) \equiv N_o(t) - N_o(t - t_{\text{obs}}), \tag{16}$$

where t_{obs} is a convenient observation time (10^3 sec) and $t_{\text{obs}} \gg t_s$. A straightforward analysis using $n_o(0) = 0$ yields

$$1 - \Delta N_o(t, t_{\text{obs}})/[(t_{\text{obs}}/t_s) n_o(\infty)] \simeq \left[\exp\left(\frac{-t}{T}\right)\right]\left[1 - \exp\left(\frac{-t_{\text{obs}}}{T}\right)\right]/(t_{\text{obs}}/T). \tag{17}$$

Results for ΔN_o are shown in Fig. 7 and are consistent with an exponential falloff with $T = 8500$ sec for times up to 10^4 sec. Note that T also determines the amplitude $[1 - \exp(-t_{\text{obs}}/T)]/(t_{\text{obs}}/T)$ in terms of t_{obs}/T. The line in Fig. 7 uses this expression with $T/t_{\text{obs}} = 8.5$. The agree-

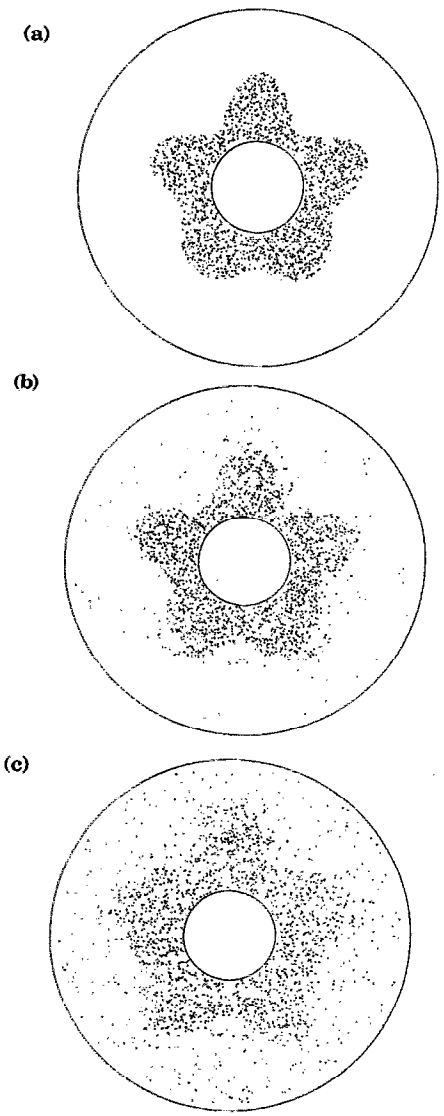

FIG. 6. Poincaré sections of 5000 sec showing the breakup of the last invariant surface with increasing b/L: (a) $b/L = 0.9$, (b) $b/L = 1.0$, and (c) $b/L = 1.1$. Here, ϵ_1, ϵ_2, and ϵ_3 have fixed values of 0.77, 0.08, and 0.15, respectively. Each Poincaré section follows 15 trajectories with starting coordinates uniformly spaced on a 12 cm radius circle.

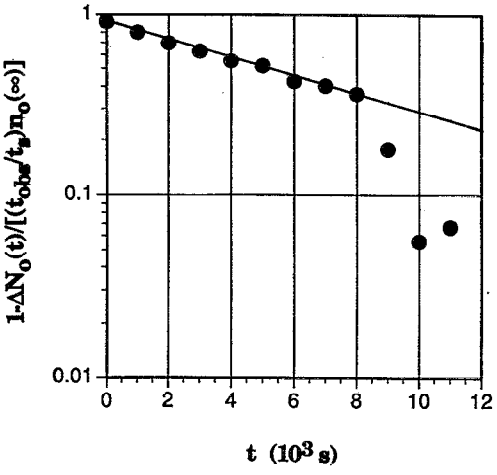

FIG. 7. An estimate for $1 - \Delta N_o(t)/[(t_{obs}/t_s)n_o(\infty)]$ vs t. The slope of this plot yields the characteristic time T for the diffusion of trajectories.

ment over the initial time range is excellent. For higher times, this simple scenario does not describe the results very well, but we do not know whether this is due to too simplistic an approach or to limited statistics.

Future experiments will be conducted to see how large a value of b/L can be obtained by varying control parameters, and b/L will be determined for the individual modes. These experiments will be conducted with a refined apparatus, now being developed, which will provide axisymmetric rather than sixfold forcing. We will obtain information on the time dependence of the velocity from hot film probes and particle tracking measurements. These detailed measurements of the dynamic as well as static properties of the flow should lead to a much improved model and should provide insight into mixing on either side of the jet as well as the possible breakup of the global barrier to mixing.

V. CONCLUSIONS

The rotating annulus experiments provide a testing ground for the study of mixing in well-controlled quasigeostrophic flows. Insights gained from the study of such a simple system with high symmetry could be applicable to the far more difficult problem of mixing in the atmosphere and oceans. One approach to the study of mixing in planetary flows is to examine the potential vorticity, as is often done in analyzing weather patterns and global circulation; potential vorticity gradients are well known to provide a barrier to mixing.[2,14] We have considered another approach, the use of the tools of Hamiltonian dynamics, which has proved to be fruitful in studying periodic and multiperiodic flows in nonrotating two-dimensional incompressible flows. Such systems can have infinitely many invariant tori that serve as barriers to both local and global transport. Our system is two dimensional as a consequence of the Taylor–Proudman theorem rather than low Reynolds number.

We have presented a simple model streamfunction (Hamiltonian) based on the experimental observations, and we have explored the behavior of the model in the context of chaotic advection. The model streamfunction does not conserve potential vorticity, but neither does the flow in the annulus for times long compared to the Ekman time[7] because of dissipation and forcing. In the experiments, rapid mixing on either side of the jet is observed for quasiperiodic (low Reynolds number) flow, but no significant transport is observed across the jet under any conditions, even at high Reynolds number, where the velocity field is turbulent. The model provides a reasonable description of the flow in the quasiperiodic regime. However, the model is not a realistic description of high Reynolds number flow where there are many excited modes and there is wave breaking. We have examined the model to see if transport across the jet occurs for any parameter values; such transport was found only for nonphysical values of b/L (values about twice as large as those observed).

Our analyses of particle streak photographs have yielded detailed information on the velocity field but no information on the time evolution of the velocity field. Future experiments will examine the dynamics of the velocity field, which should lead to an improved model streamfunction. Future analyses of transport for streamfunctions deduced either from experiment or from direct solution of the Navier–Stokes equation should exploit tools from Hamiltonian dynamics such as the Chirikov overlap criterion[15] to gain insight into both local and global mixing.[16,17]

ACKNOWLEDGMENTS

We thank Donny Goff and Bill Craven for help in the programming, Joel Sommeria for his participation in this research program, and Dwight Barkley, Diego del Castillo-Negrete, Philip Morrison, Lorenzo Polvani, and Philip Marcus for helpful discussions.

This work was supported by the Office of Naval Research Nonlinear Dynamics Program, Grant No. N00014-89-J1495. RPB gratefully acknowledges the hospitality of the Center for Nonlinear Dynamics of the University of Texas, and support for continuing this work from the National Science Foundation under Low Temperature Physics Grant No. DMR-8714862.

[1] M. E. McIntyre, J. Atmos. Terr. Phys. **51**, 29 (1989).
[2] J. Pedlosky, *Geophysical Fluid Dynamics* (Springer-Verlag, New York, 1987), 2nd ed.
[3] H. Aref, J. Fluid Mech. **143**, 1 (1984).
[4] See, for example, the reviews of J. M. Ottino, Annu. Rev. Fluid Mech. **22**, 207 (1990); *The Kinematics of Mixing: Stretching, Chaos, and Transport* (Cambridge U.P., Cambridge, 1989).
[5] An exception is the study of advection beyond the transition to oscillating Rayleigh–Benárd convection: T. H. Solomon and J. P. Gollub, Phys. Rev. A **38**, 6280 (1990).
[6] A global barrier to mixing in a cavity can, however, be seen in Fig. 11(a) of C. W. Leong and J. M. Ottino, J. Fluid Mech. **209**, 463 (1989).
[7] J. Sommeria, S. D. Meyers, and H. L. Swinney, Nature **337**, 58 (1989).
[8] J. Sommeria, S. D. Meyers, and H. L. Swinney, in *Nonlinear Topics in Ocean Physics*, edited by A. Osborne (North-Holland, Amsterdam, 1991).
[9] S. D. Meyers and H. L. Swinney, in *Nonlinear Structures in Dynamical Systems*, edited by L. Lam and H. C. Morris (Springer-Verlag, New York, 1990), p. 166.
[10] A slightly different form of correction for the boundary layer function was used in Fig. 6.

[11] R. S. MacKay, J. D. Meiss, and I. C. Percival, Phys. Rev. Lett. **52**, 697 (1984).
[12] D. Bensimon and L. P. Kadanoff, Physica D **13**, 82 (1984).
[13] The coordinates (r,ϕ) are not canonically conjugate, but a simple transformation to coordinates $(J,\phi) = (\frac{1}{2}r^2,\phi)$ provides a canonically conjugate pair.
[14] M. N. Juckes and M. E. McIntyre, Nature **328**, 590 (1987).
[15] B. V. Chirikov, J. Nucl. Energy C **1**, 253 (1960).
[16] D. del Castillo-Negrete and P. Morrison (private communication).
[17] L. M. Polvani and J. Touma, in *Nonlinear Phenomena in Atmospheric and Oceanic Sciences*, edited by G. Carnevale and R. Pierrehumbert (Springer-Verlag, New York, 1991).